Science Advances
AAAS

Supplementary Materials for

Insights into the evolution of enzymatic specificity and catalysis: From Asgard archaea to human adenylate kinases

Apoorv Verma *et al.*

Corresponding author: Elisabeth Sauer-Eriksson, elisabeth.sauer-eriksson@umu.se;
Magnus Wolf-Watz, magnus.wolf-watz@umu.se

Sci. Adv. **8**, eabm4089 (2022)
DOI: 10.1126/sciadv.abm4089

This PDF file includes:

Supplementary Text

Quantification of microscopic rate constants from ^{19}F spin relaxation

Relaxation dispersion experiments can provide accurate quantification of parameters that define a conformational exchange process. Here the attention is focused on the dynamic interconversion between open and closed OdinAK that occurs during turn-over conditions. Under favorable conditions and assuming a two-state model, parameters defining (i) kinetics (k_{ex}, k_{close}, k_{open}), (ii) thermodynamics (p_A *and* p_B) and (iii) structural information (chemical shifts, δω) can be quantified. Here the parameters of interest are the microscopic rate constants that are associated with closing (k_{close}) and opening (k_{open}) of OdinAK during turn-over conditions. For a two-state process with exchange between open and closed states the exchange is described by; $k_{ex} = k_{close} + k_{open}$, where $k_{close} = p_B k_{ex}$ and $k_{open} = p_A k_{ex}$. The exchange parameters (k_{ex}, p_A and δω) can be fitted directly to relaxation dispersion profiles if the exchange occurs on an intermediate time-scale, where the time-scale is defined by the difference in chemical shifts for the exchanging states. With such as complete characterization also the microscopic rate constants k_{close} and k_{close} can be fitted directly from the dispersion profiles. A common scenario that also applies to OdinAk, is the so called "fast exchange" regime where the exchange process (k_{ex}) is much faster than the difference in chemical shift (δω). In the fast-exchange regime the parameters that can be fitted are k_{ex} (here $k_{ex} = k_{close} + k_{open}$) and the exchange-product $\frac{p_A p_B (\delta\omega)^2}{k_{ex}}$, where p_A, p_B, and δω correspond to populations of the exchanging states and the difference in chemical shift (in rad/s) between the exchanging states, respectively. The dispersion profiles for OdinAK with saturating amounts of ADP and Mg^{2+} has the typical mono-exponential shape that is signifying exchange dynamics in the fast-exchange regime and consequently it is only possible to fit k_{ex} and the "exchange product", $\frac{p_A p_B (\delta\omega)^2}{k_{ex}}$. It is possible to extract the components p_A, p_A and k_{ex} from the exchange-product if the chemical shift difference (δω) can be quantified from an independent experiment. To this end, we postulate that the X-ray structures of apo and Ap5A bound OdinAK represent the open and closed states at the extremes of the catalytic cycle. Therefore, the chemical shifts difference between these states (δω) can be measured directly from their corresponding ^{19}F spectra (**fig. S11**). By using this information on the chemical shift difference we are able to compute the microscopic opening and closing rate constants according to; $k_{close} = p_B k_{ex}$ and $k_{open} = p_A k_{ex}$.

Supplementary Tables

Table S1. Data collection and refinement statistics for OdinAK complexes.

Data-collection statistics	OdinAK-apo	OdinAK-Ap5A	OdinAK-GTP
Synchrotron/Beamline	MaxIV/BioMax	PETRA/P13	MaxIV/BioMax
Space group	$P2_12_12_1$	$P2_12_12_1$	$P2_12_12_1$
Unit-cell parameters (Å,°)	77.8, 77.8, 217.6 90.0, 90.0, 90.0	69.78, 143.16, 158.71 90.0, 90.0, 90.0	77.61, 78.79, 218.19 90.0, 90.0, 90.0
Resolution limits[a] (Å)	49.08-1.85 (1.88-1.85)	71.58-2.75 (2.85-2.75)	49.27-2.50 (2.59-2.50)
No. of unique reflections	113276 (11096)	42150 (4139)	46829 (4562)
Multiplicity	13.6 (13.7)	13.1 (12.5)	6.8 (6.7)
Completeness (%)	100.0 (100.0)	100.0 (100.0)	99.7 (98.5)
R_{merge}	0.116 (2.028)	0.135 (1.981)	0.142 (0.880)
R_{PIM}	0.047 (0.813)	0.056 (0.846)	0.088 (0.548)
$\langle I/\sigma (I)\rangle$	11.7 (1.4)	9.3 (1.2)	8.2 (2.0)
CC1/2	1.00 (0.65)	0.99 (0.63)	0.99 (0.71)
Wilson B-factor (Å^2)	32	83	41
R factor (%)	0.204 (0.303)	0.238 (0.370)	0.198 (0.310)
R free (%)	0.248 (0.357)	0.272 (0.414)	0.259 (0.391)
No. of protein atoms	9591	9335	9446
No. of water molecules	475	-	153
No. of ligand atoms	8	342	192
Bond length (Å)	0.014	0.006	0.014
Bond angles (°)	1.27	1.17	1.40
Clash score	5	13	6
Ramachandran: Residues in m favored regions (%)	97	97	97
Ramachandran: Residues in disallowed regions (%)	0.0	0.0	0.2
Average B-factor protein (Å^2)	46	93	51
Average B-factor ligands (Å^2)	57	97	93
Average B-factor solvent (Å^2)	42	-	36
PDB ID	7OWH	7OWE	7OWJ

[a]Values in parenthesis are for the high-resolution shell. Resolution limits were determined by applying a cut-off based on the mean intensity correlation coefficient of half-datasets, CC1/2.

Table S1 (continued). Data collection and refinement statistics for OdinAK complexes.

Data-collection statistics	OdinAK-dTTP	OdinAK-CTP
Synchrotron-Beam line	MaxIV/BioMax	MaxIV/BioMax
Space group	$P2_12_12_1$	$P2_12_12_1$
Unit-cell parameters (Å,°)	76.82, 77.20, 214.75	76.49, 77.63, 216.88
	90.0, 90.0, 90.0	90.0, 90.0, 90.0
Resolution limits[a] (Å)	44.08-3.10 (3.21-3.10)	15.01-2.90 (3.08-2.90)
No. of unique reflections	23925 (2363)	29184 (2878)
Multiplicity	13.2 (13.0)	8.9 (9.0)
Completeness (%)	100.0 (100.0)	99.3 (100.0)
R_{merge}	0.356 (3.017)	0.315 (1.732)
R_{PIM}	0.144 (1.229)	0.163 (0.904)
$<I/\sigma (I)>$	9.1 (2.3)	5.5 (2.1)
CC1/2	0.99 (0.49)	0.99 (0.63)
Wilson B-factor (Å^2)	76	66
R factor (%)	0.218 (0.295)	0.199 (0.271)
R free (%)	0.263 (0.359)	0.256 (0.359)
No. of protein atoms	9384	9345
No. of water molecules	6	27
No. of ligand atoms	174	174
Bond length (Å)	0.007	0.004
Bond angles (°)	1.05	0.59
Clash score	11.2	4.9
Residues in most favored regions (%)	95	97
Residues in disallowed regions (%)	0.1	0.0
Average B-factor protein (Å^2)	70	67
Average B-factor ligands (Å^2)	73	93
Average B-factor solvent (Å^2)	45	47
PDB ID	7OWK	7OWL

Table S2. Exchange parameters obtained from OdinAK Y44W ^{19}F CPMG relaxation dispersion at 65 °C.

Substrates (+ Mg^{2+})	δω* (s^{-1})	k_{ex} (s^{-1})	C= P_{open} P_{closed} $\delta\omega^2$ (s^{-2})
ADP	357	1476 ± 99	40452 ± 3600
ATP + AMP	357	1360 ± 109	42350 ± 4300
GTP + AMP	357	1324 ± 70	71806 ± 5700
CTP + AMP	357	1495 ± 76	73390 ± 5300
UTP + AMP	357	1403 ± 106	63162 ± 3800
dTTP + AMP	357	1409 ± 93	67064 ± 5300

* δω is the ^{19}F chemical shift difference between Y44W apo (open) and Ap5A (closed) states

Supplementary Figures

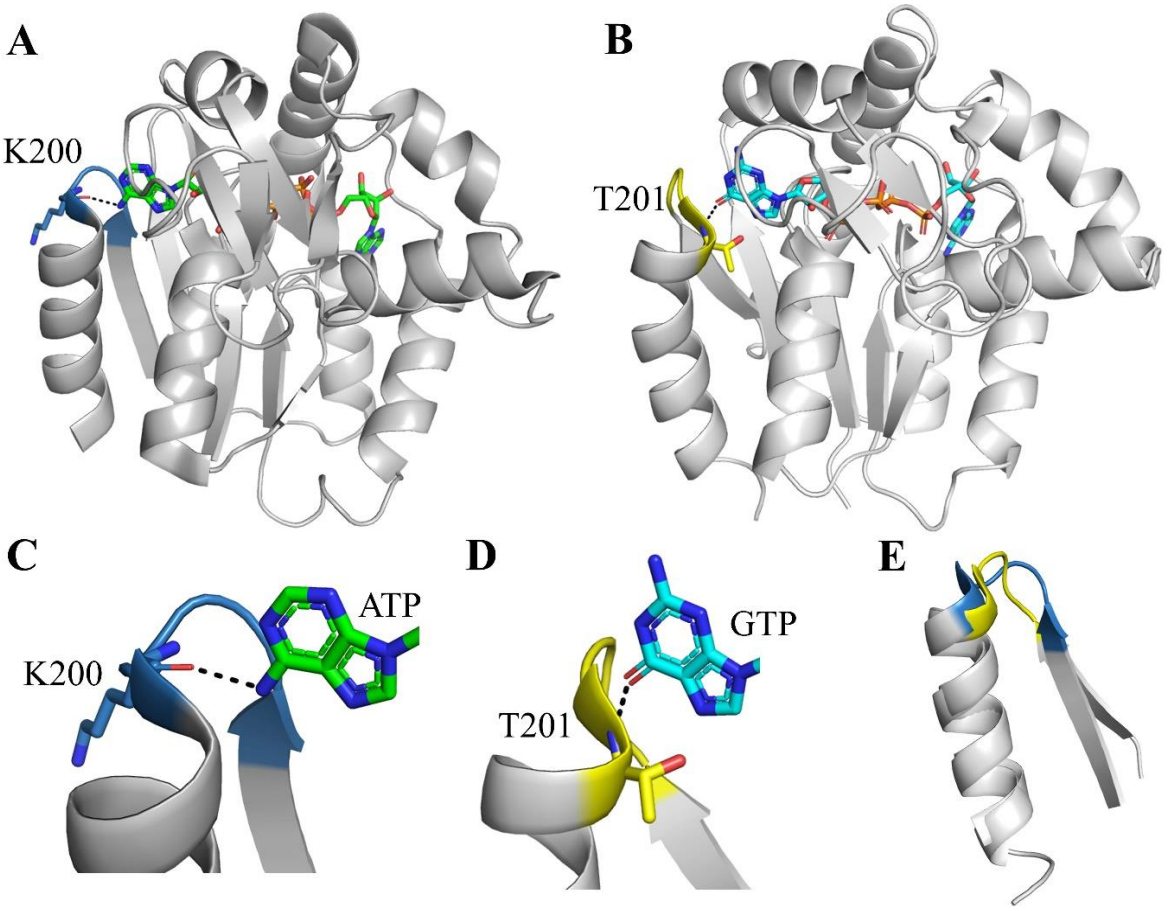

Fig. S1. **ATP and GTP "selectivity loops".** Selectivity for ATP or GTP in the NMP kinase family can be predicted from the orientation of the selectivity loop as illustrated for *E. coli* adenylate kinase and human AK3. (**A**) Structure of ATP specific *E. coli* adenylate kinase (AK_{eco}) in complex with the inhibitor Ap5A (PDB ID:1AKE) (*9*). The selectivity loop is colored in blue. (**B**) Structure of the GTP specific human AK3 in complex with the inhibitor Gp5A (PDB ID: 6ZJB) (*7*). The selectivity loop is colored in yellow. (**C**) Zoom in on the ATP specific selectivity loop showing the key hydrogen bond formed between the adenosine base of ATP and the backbone oxygen of K200. (**D**) Zoom in on the GTP specific selectivity loop with the key hydrogen bond formed between the guanosine base of GTP and the backbone amide hydrogen of T201. (**E**) Overlay of the ATP and GTP specific selectivity loops of AK_{eco} and human AK3.

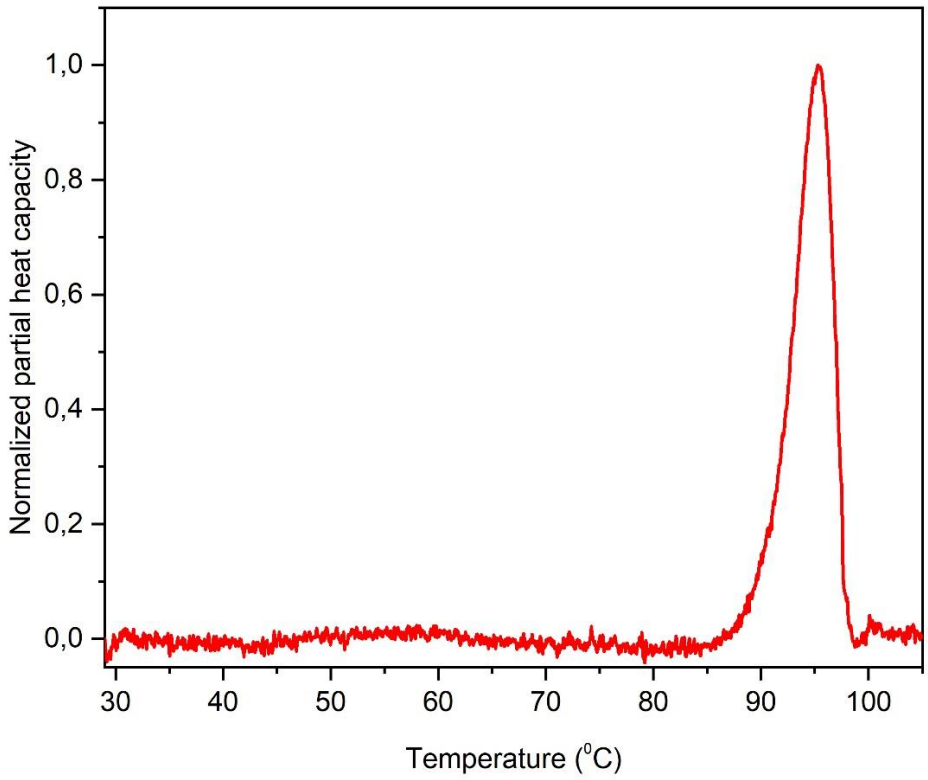

Fig. S2. **Thermal stability of OdinAK with ATP and $MgCl_2$.** The thermal stability of OdinAK supplemented with 630 µM ATP and 5 mM $MgCl_2$ was followed with differential scanning calorimetry. The T_m was determined from the maximum of the thermogram and was found to be 95 °C. The data has been corrected with the solvent background and the normalized partial heat capacity is displayed.

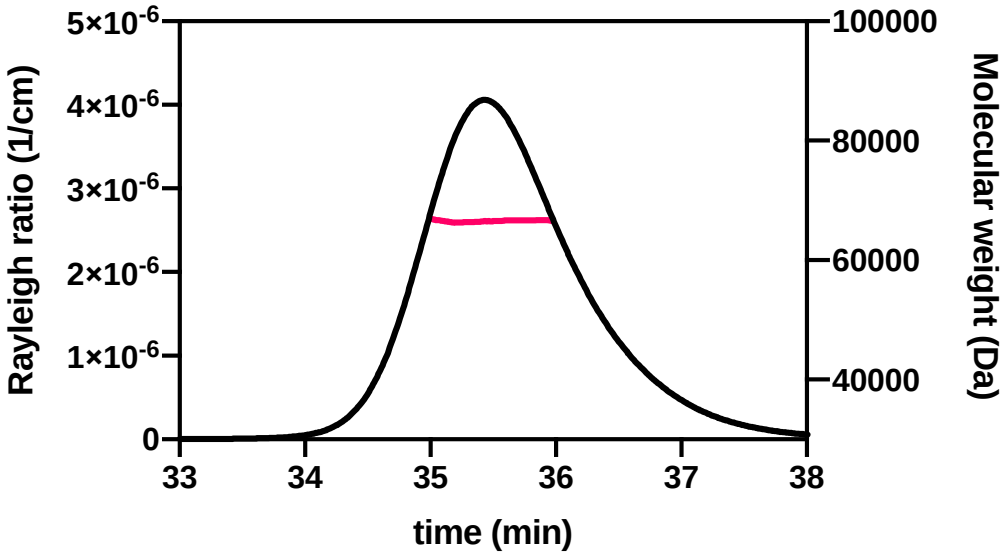

Fig. S3. **SEC-MALS of trimeric OdinAK.** The size exclusion chromatogram shows the Rayleigh ratio which is directly proportional to the intensity of the scattered light in excess to the solvent (left y-axis). The red line indicates the calculated molecular weight (69 ± 5 kDa.) of the protein throughout the peak (scale on the right y-axis). The molecular weight of the monomer and trimer calculated from the primary sequence is equal to 23 and 69 kDa, respectively.

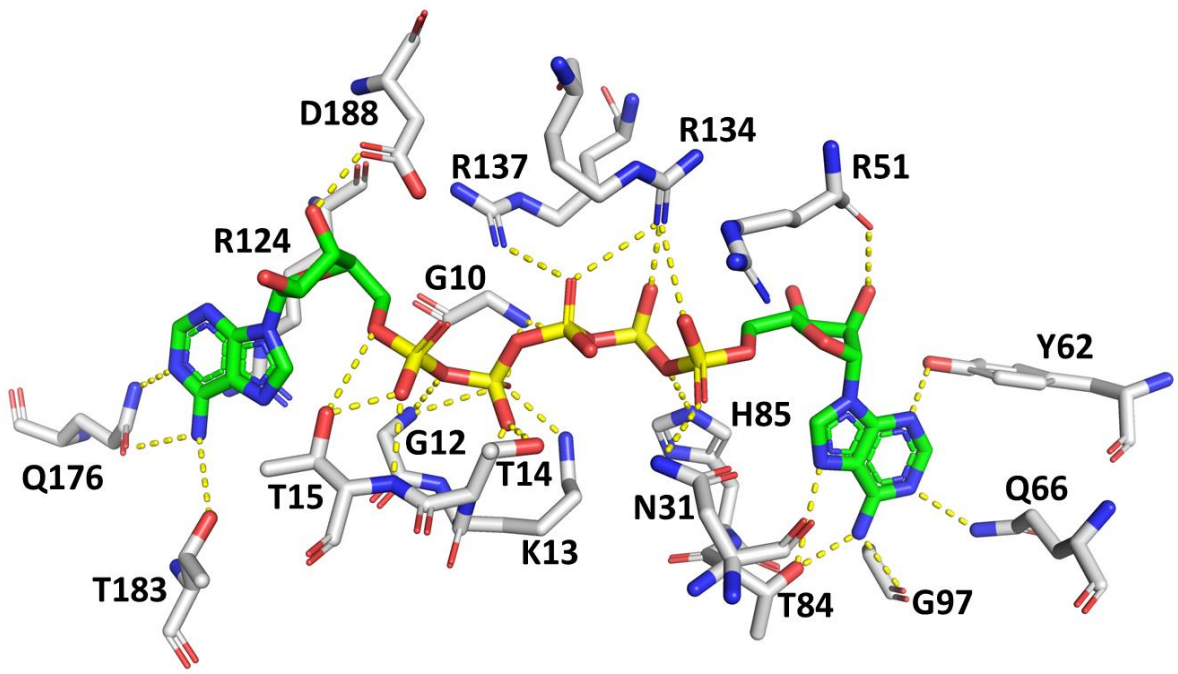

Fig. S4. ATP and AMP binding sites in OdinAK. Residues in OdinAK that are responsible for the binding and recognition of substrates are illustrated from the crystallographic structure solved in complex with the inhibitor Ap5A. The binding sites to the left and right correspond to the specific recognition of ATP and AMP, respectively. The identity of substrate interacting residues are indicated.

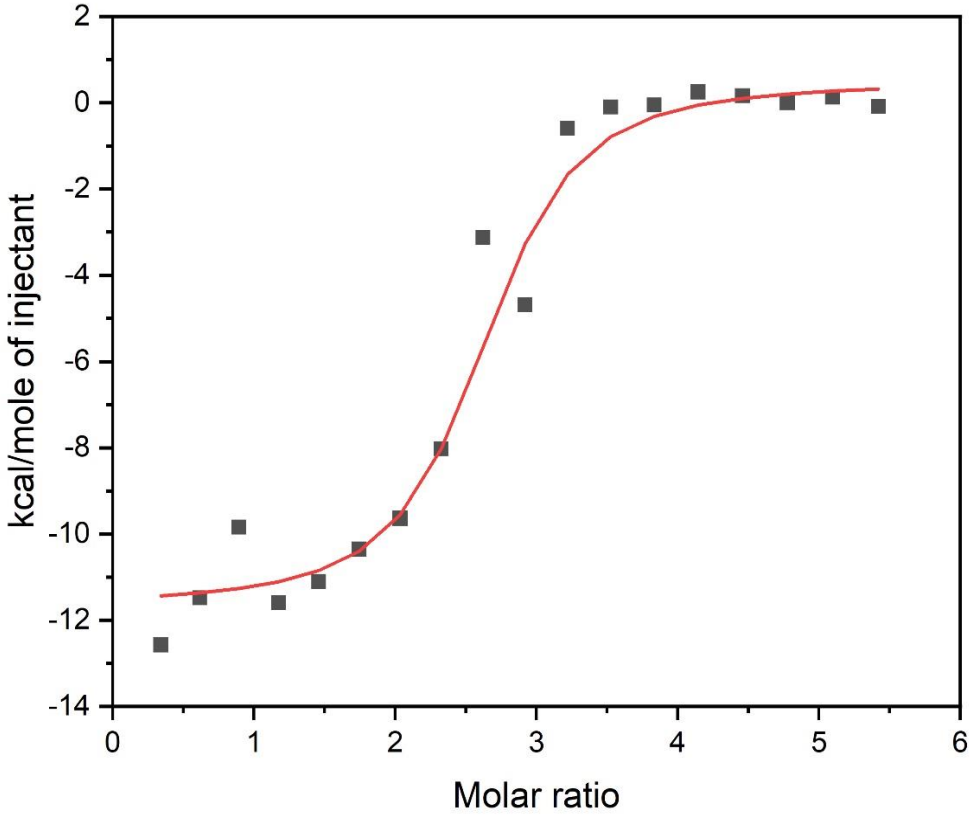

Fig. S5. **ITC titration isotherm between OdinAK and ATP with Mg^{2+}.** Binding affinities (K_d) (**Table 1**) were quantified at 25 °C with ATP, 5mM Mg^{2+} and 27 µM of OdinAK trimer using isothermal titration calorimetry. The fitted binding isotherms for "one set of sites" model is shown as a red line. The molar ratio shown on basis of trimer concentration and therefore the molar ratio (N) of 3 indicates binding of three molecules of ATP to one OdinAK trimer.

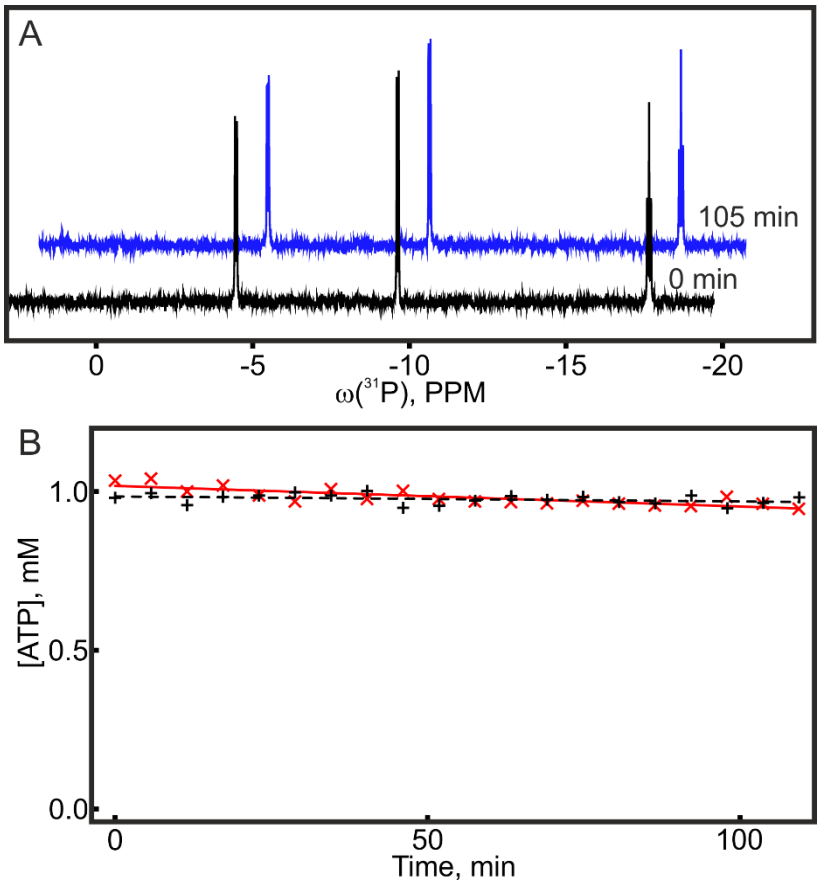

Fig. S6. Water mediated ATP hydrolysis is suppressed by OdinAK at 65 ºC. (**A**) ^{31}P NMR spectrum of ATP in the presence of 300 nM of OdinAK and 5 mM $MgCl_2$ at OdinAK addition and after 105 min, a typical experiment time for the ^{31}P NMR assay. No ADP or inorganic phosphate can be detected. (**B**) Determined concentrations of ATP during the experiment. The red and the black series is two independent measurements. A small decrease in concentration, $2*10^{-2}$ ATP molecules per second and OdinAK molecule was detected. This slow depletion of ATP is not significant when comparing to the adenylate kinase reaction.

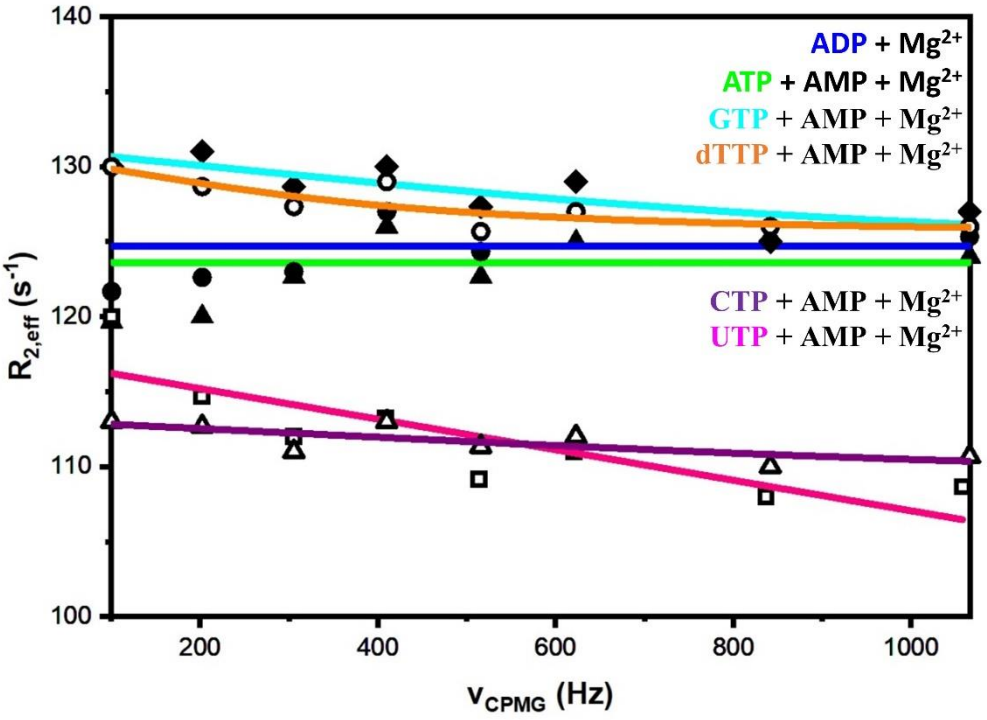

Fig. S7. ^{19}F CPMG relaxation dispersion profiles obtained from wild-type W174 at 65 °C. Wild-type tryptophan W174 in OdinAK yielded flat (or close to flat) dispersion profiles with all NTP's together with Mg^{2+} and AMP (i.e. turn-over conditions) and therefore did not report conformational dynamics on the CPMG time scale.

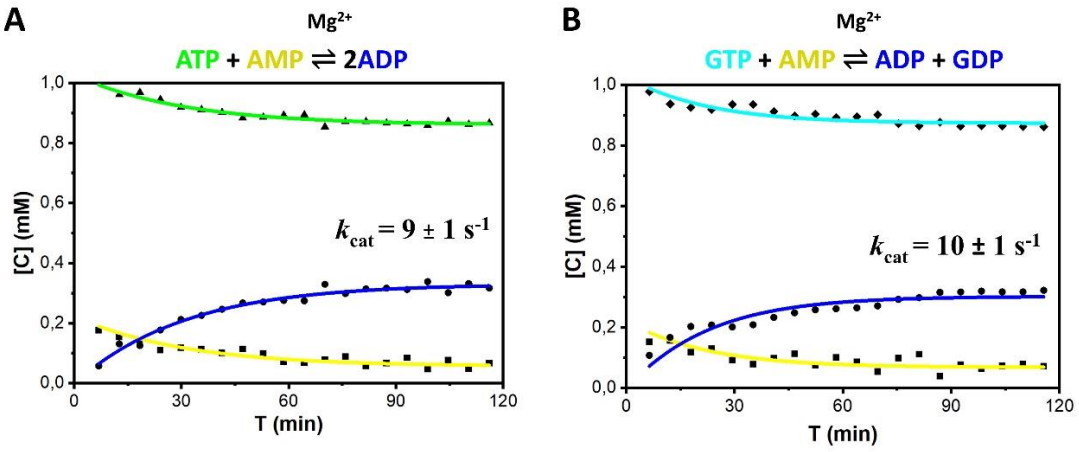

Fig. S8. **Enzyme kinetics of the OdinAK Y44W variant from ^{31}P NMR at 65 °C.** The Y44W mutant exhibited similar catalytic activity (k_{cat}) for ATP (**A**) and GTP (**B**) as the wild-type and was therefore used for ^{19}F NMR studies.

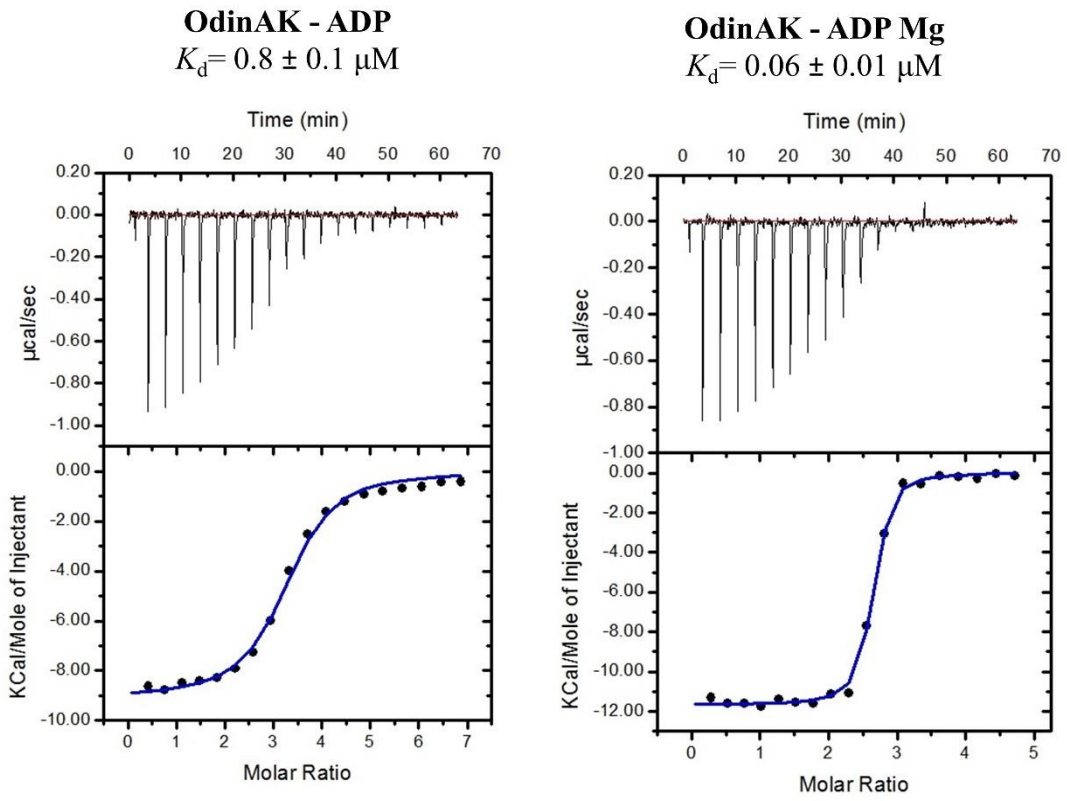

Fig. S9. **ITC titration isotherms between OdinAK and ADP ± Mg^{2+}.** Binding affinities (K_d) were quantified at 25 °C using isothermal titration calorimetry (**Table 1**). The fitted binding isotherms for "one set of sites" model are shown. . The concentration of OdinAK is shown on basis of trimer concentration and therefore the molar ratio (N) of 3 indicates binding of three molecules of NTP to one OdinAK trimer. Left: quantification of binding between OdinAK and ADP. Right: quantification of binding between OdinAK and ADP in the presence of 5 mM Mg^{2+}.

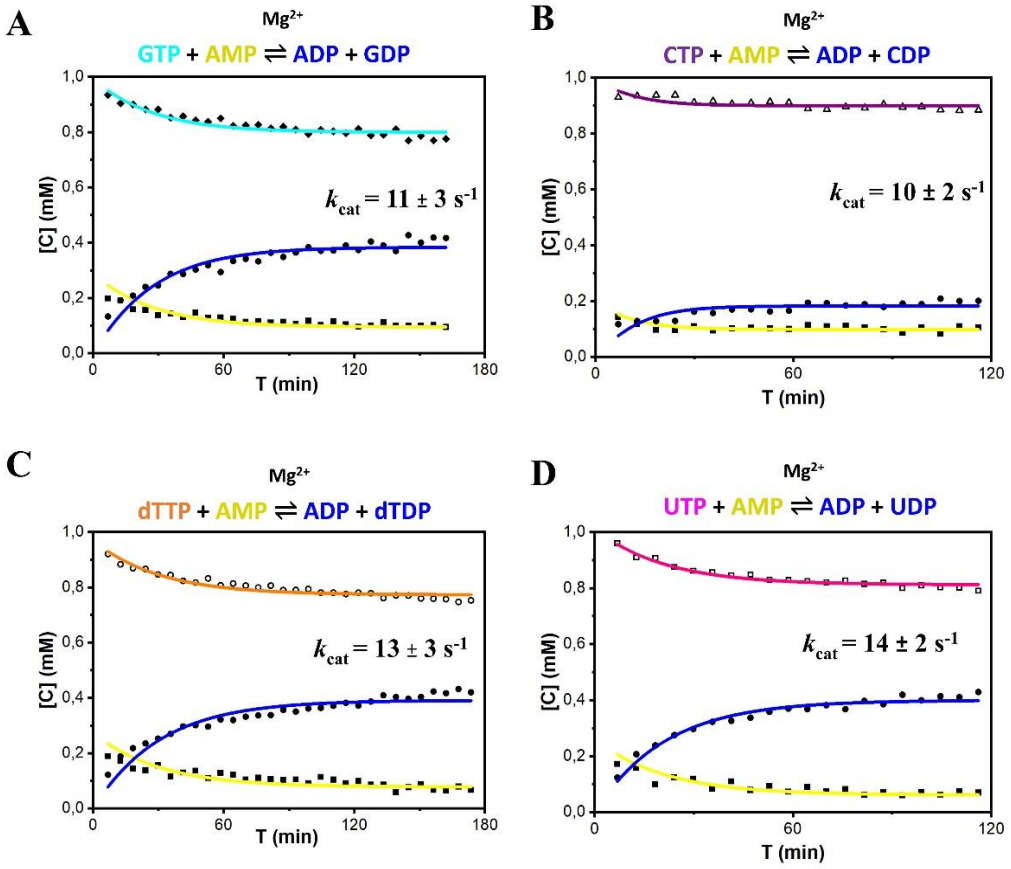

Fig. S10. Quantification of OdinAK catalysis with different NTP substrates. (**A**) GTP, (**B**) CTP, (**C**) dTTP, and (**D**) UTP. The catalytic activity (k_{cat}) was quantified using ^{31}P NMR assay (see **Fig. 3D** for results with ATP). The experiment was performed with the indicated NTP together with AMP and Mg^{2+} at 65 °C.

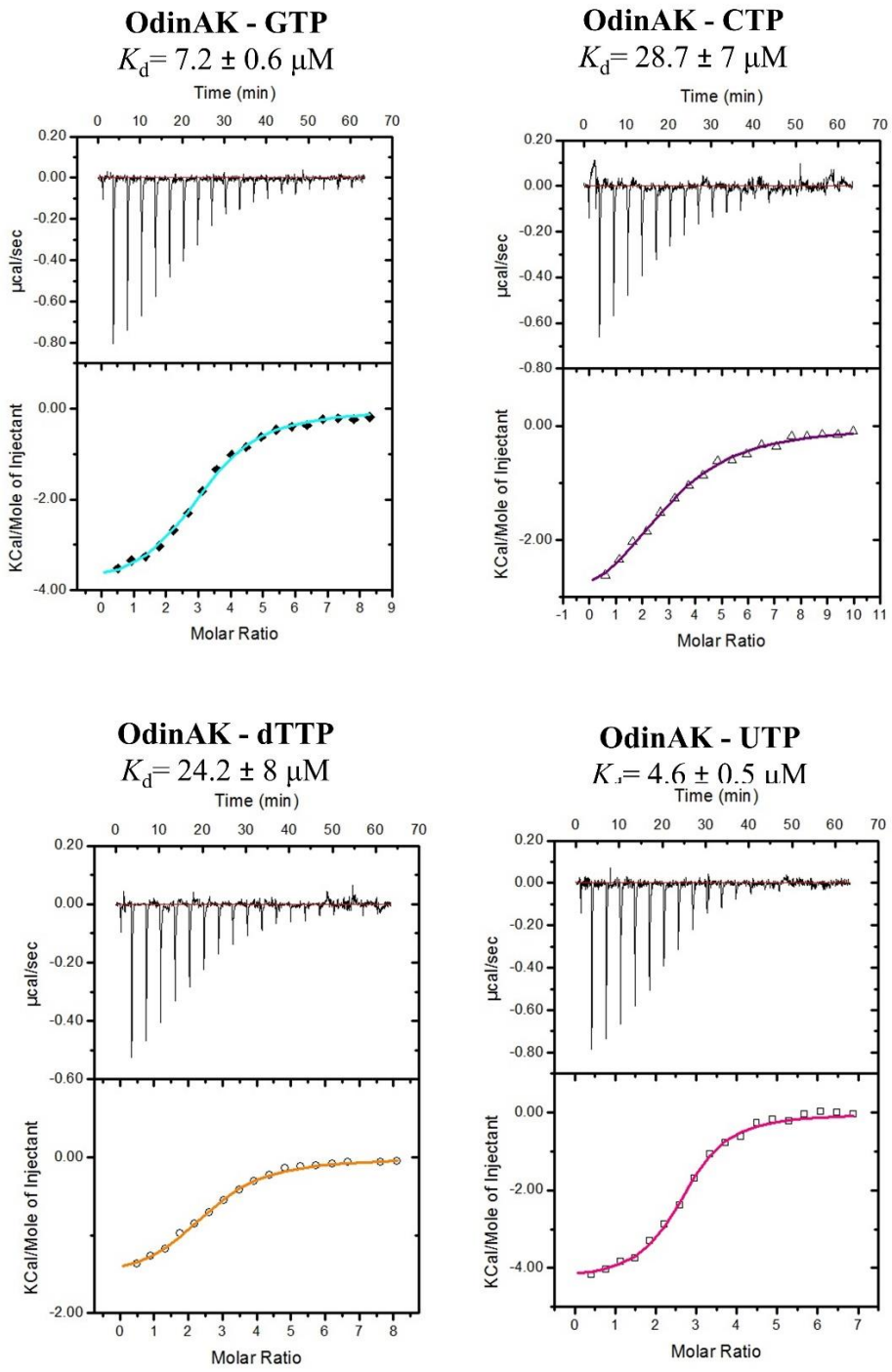

Fig. S11. **Quantification of NTP binding affinities for OdinAK**. Binding affinities (K_d) for different NTP substrates (as indicated) were quantified at 25 °C using isothermal titration calorimetry (**Table 1**). The fitted binding isotherms for "one set of sites" model are shown. The concentration of OdinAK is shown on basis of monomer concentration and therefore the molar ratio (N) of 3 indicates binding of three molecules of NTP to one Odin trimer.

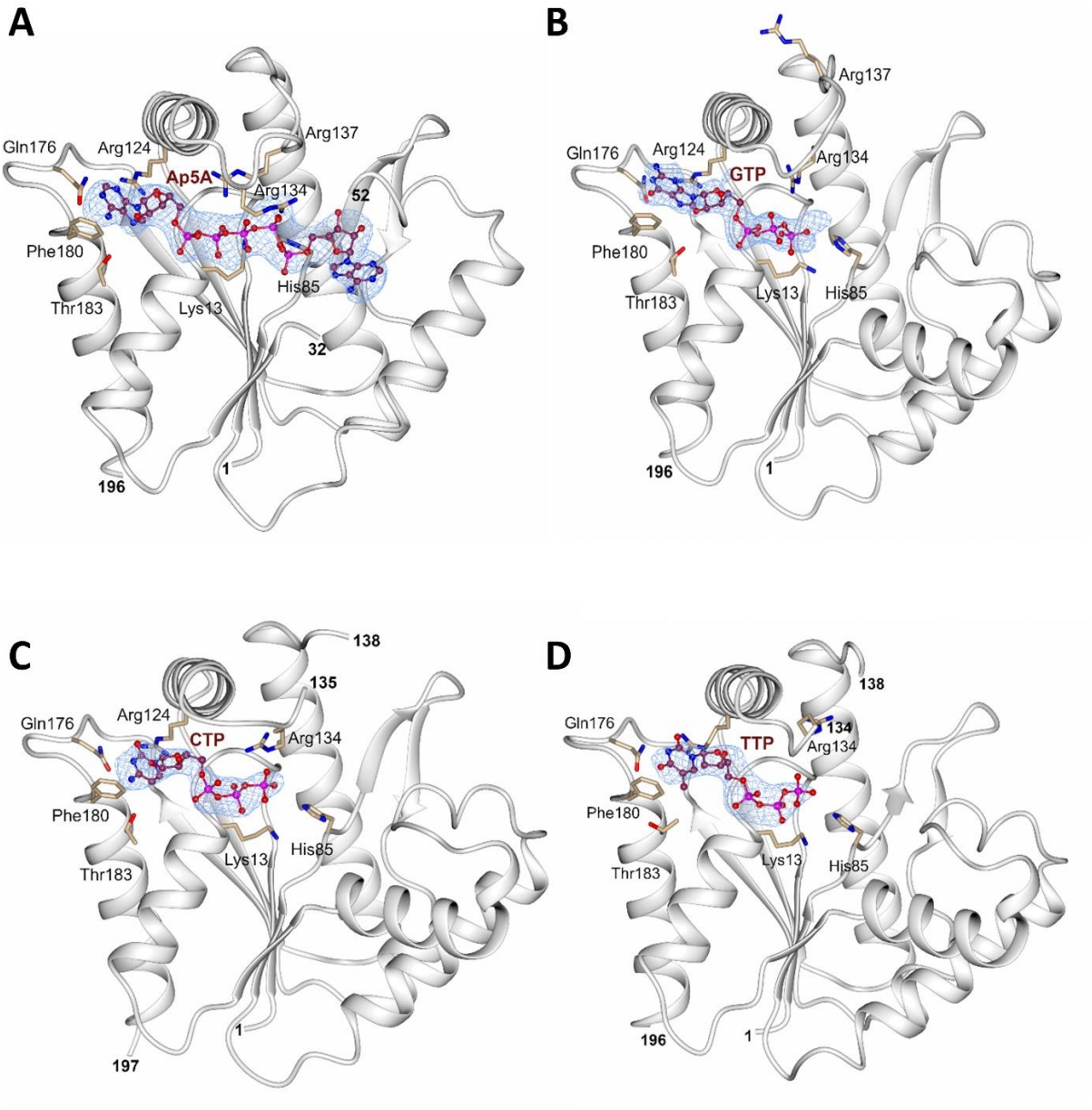

Fig. S12. Representative electron density covering the refined model of nucleotides. An unbiased difference (|Fo|-|Fc|) electron density map contoured at three times the RMS value of the map is shown in blue for monomer A. To reduce model bias, the nucleotide molecule was excluded from the coordinate file that was subjected to refinement before calculation of the electron density map. Key

residues involved in the catalysis and substrate recognition are shown as sticks. In the figure of the OdinAK-Ap5A complex structure residues 33-37 have been removed for clarity. (**A**) OdinAK-Ap5A. (**B**) OdinAK-GTP. (**C**) OdinAK-CTP. (**D**) OdinAK-TTP.

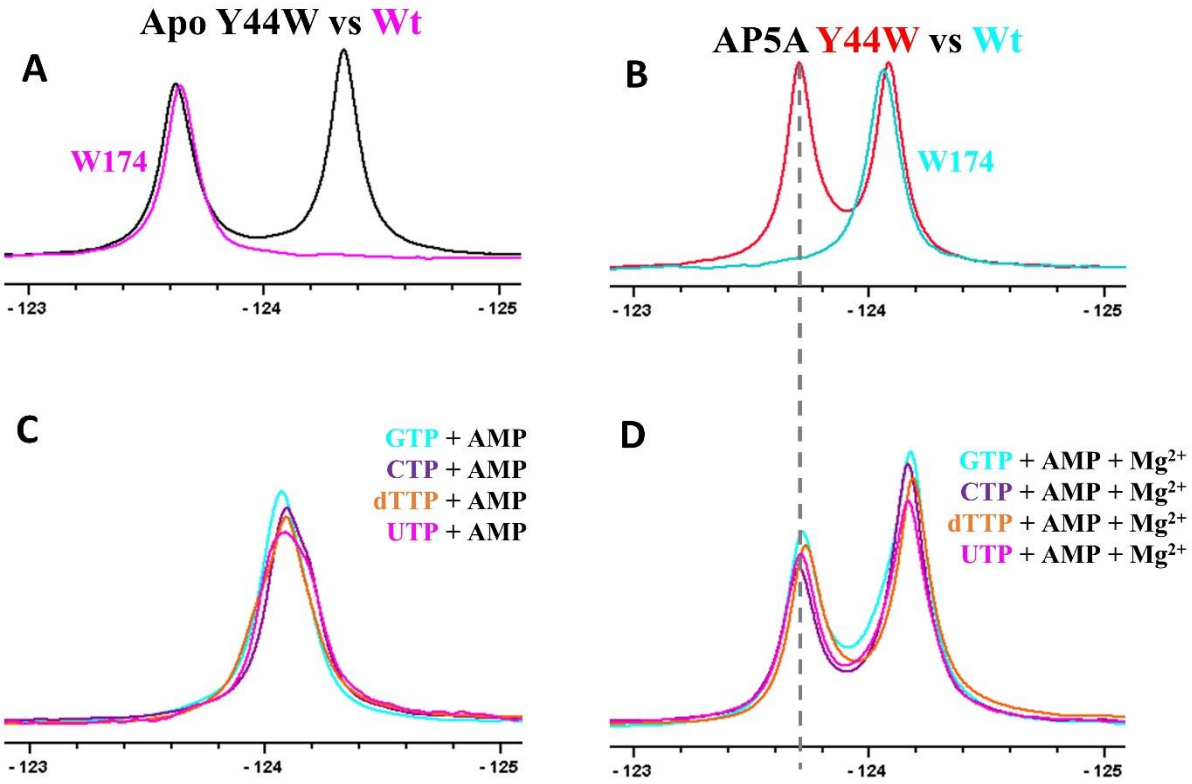

Fig. S13. **^{19}F NMR of the OdinAK Y44W mutant at 65 °C. (A-B)** Assignment of the peaks (Y44W and W174) was done by comparing the spectra of mutant Y44W and wild type (WT) OdinAK in both open (apo) and closed (Ap5A-bound) states. The chemical shift difference (δω) between open and closed states of OdinAK (**table S2**) was obtained from Y44W apo (black) and Ap5A (red) spectra, and used for CPMG RD analysis. **(C-D)** Substrates, GTP, CTP, dTTP, and UTP follow the same pattern upon titration, NTP 1:10 + AMP 1:10 (+ 5 mM Mg^{2+}) are shown.

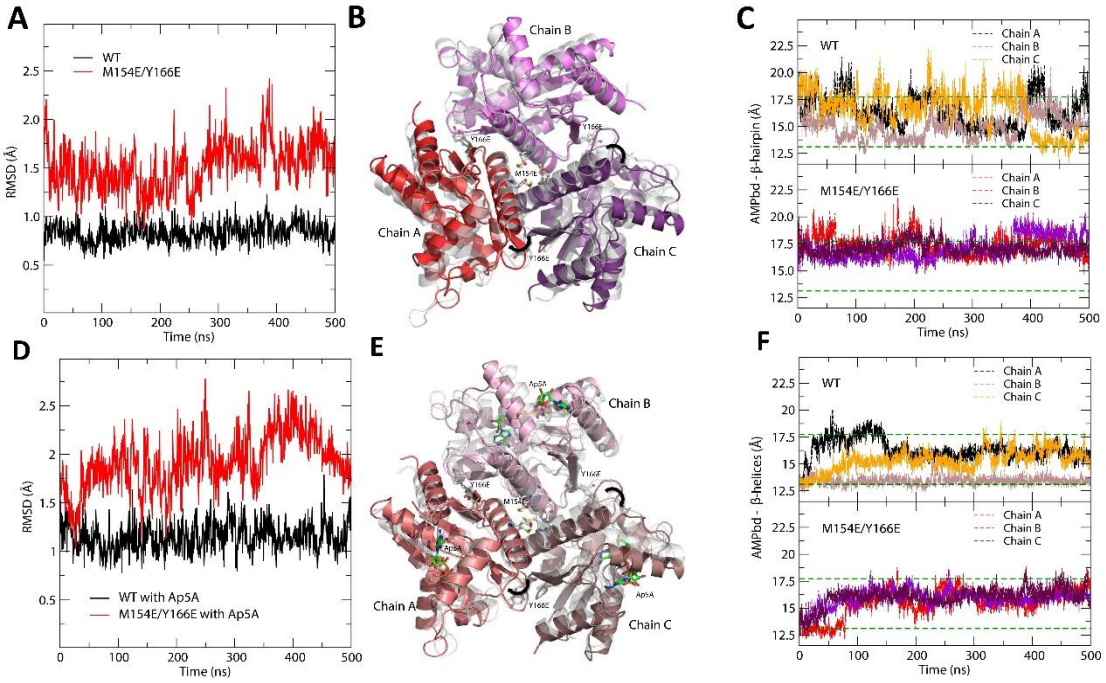

Fig. S14. Molecular dynamics simulations of OdinAK with and without Ap5A. Panels (**A**)-(**C**) are for the substrate-free system and panels (**D**)-(**F**) are for the systems with bound Ap5A. (**A**) The RMSD of the trimerization helices between wild-type (black) and V1 OdinAK variant (red) in the absence of Ap5A. (**B**) Average structures of the MD simulations (between 400 ns and 500 ns) for the wild-type (transparent gray) and V1 variant of OdinAK (red: Chain A; purple: Chain B; violet: Chain C). The arrow indicates the outward tilting of the trimerization helices in the V1 variant, which results in a larger RMSD in (**A**). (**C**) The change in AMPbd – β-hairpin distance during MD simulations. In each panel, the green dashed lines show the corresponding distances of substare-free (upper line) and Ap5A-bound OdinAK (lower line), respectively. (**D**) The RMSD of the trimerization helices between wild-type and V1 variant with bound Ap5A. (**E**) Average structures of the MD simulations (between 400 ns and 500 ns) for the wild-type (transparent gray) and V1 OdinAK variant (deep salmon: Chain A; light pink: Chain B; dirty violet: Chain C). (**F**) The change in AMPbd – β-hairpin distance during MD simulations. Similar to the substrate-free case, the AMPbd slowly opens in all three chains of the V1 variant with Ap5A.

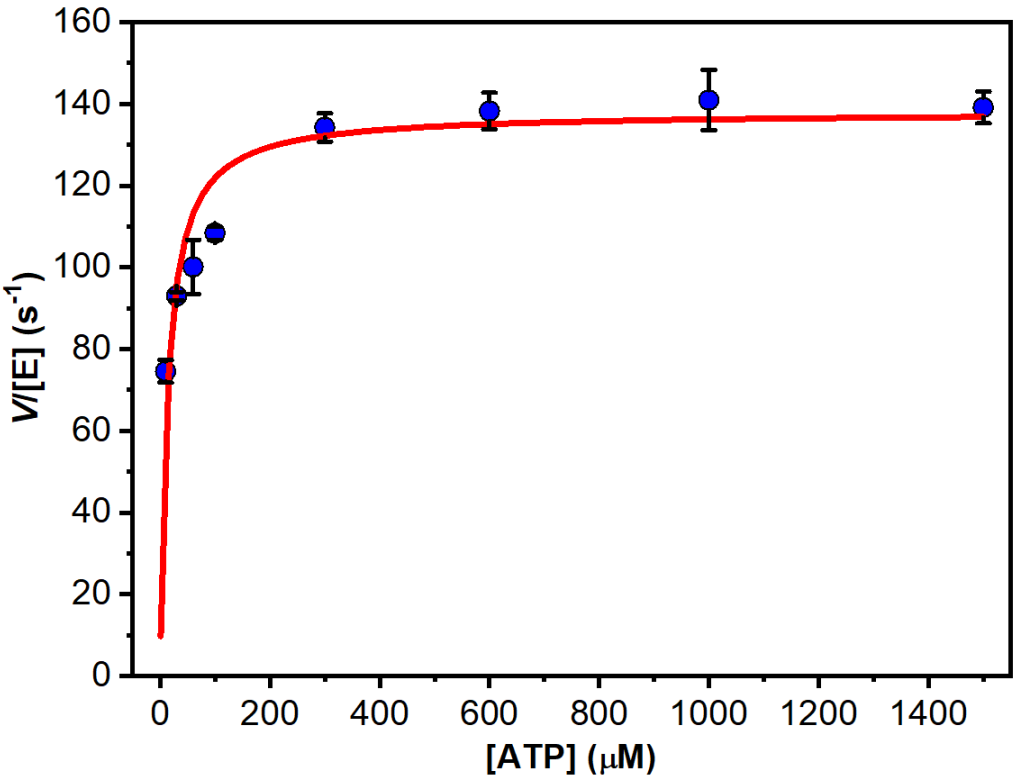

Fig. S15. **Enzymatic activity of AK1**. The catalytic parameters of AK1 (k_{cat} and K_M) were obtained by fitting the reaction velocity for production of ADP from ATP and AMP against a variation in ATP concentration with AMP fixed at 300 μM. The reaction velocity was scaled with the total enzyme concentration and the Michaelis-Menten equation (Equation 1 in Materials and Methods) was fitted to the data. The k_{cat} and K_M at 25 ºC were found to be 140 ± 8 s^{-1} and 13 ± 4 μM, respectively.

A

```
OdinAK 4    ILTGVPGAGKTTVCNKLAEKMSNLSVVNYGDVIFEE  39
            +LTG PG GKTT+  +LA K S L  +N GD+  EE
hAK6   7    LLTGTPGVGKTTLGKELASK-SGLKYINVGDLAREE  41
```

OdinAK

MRF**ILTGVPGAGKTTVCNKLAEKMSNLSVVNYGDVIFEE**AKKLYPSIIQVREDTRKLPRADYRNIQIEAAKKISLITDNLIVDTHM
SLKTPYGFYPGLIPETINIIQPDGIILLEFNPRDVIARREKDRLAGKRVTRDMESETDILLHQQVNRMFAVSYSAINQCYVKIIDLT
WPQEYEFQHTEYAVNKIIEMLNFKI

hAK6

M**LLPNILLTGTPGVGKTTLGKELASKSGLKYINVGDLAREE**QLYDGYDEEYDCPILDEDRVVDELDNQMREGGVIVDYHGCDFFPE
RWFHIVFVLRTDTNVLYERLETRGYNEKKLTDNIQCEIFQVLYEEATASYKEEIVHQLPSNKPEELENNVDQILKWIEQWIKDHNS

Fig. S16. **BLAST result from OdinAK and hAK6**. Result from a BLAST search with OdinAK as query against the human proteome in UniProt. The top hit was hAK6 with 19 identical residues over a 36 amino acid segment. Top: the aligned segments from the BLAST search with conserved and similar amino acid residues indicated in the middle row. Bottom: The aligned sequences (yellow for OdinAK and gray for hAK6) are displayed on the full amino acid sequences.